2021 43rd Annual International Conference of the
IEEE Engineering in Medicine & Biology Society (EMBC)
Oct 31 - Nov 4, 2021. Virtual Conference

Distributed Capacitors for MR-Receive-Coils: Theory and Method

Enrico Pannicke[1,3], Oliver Speck[2,3], Ralf Vick[2]

***Abstract*— MR coils are a crucial part in the receiving chain of an MRI. Their characteristics determine the signal-to-noise-ratio (SNR) as well as the quality of the illumination of the volume-of-interest (VOI), which is significantly reduced as the circumference of the conductor is comparable in size to the wavelength.**
A well-known countermeasure to this is the use of distributed capacitors on the circumference of conductor loops. Although this measure is mentioned in numerous works, there is no systematic framework to correctly determine the values of these capacitors. In this work a systematic framework for the analysis of distributed capacitors on conductor loops is established. This is achieved by a four-pole representation of the circular loop, which allows for a eigen-mode analysis to determine the correct values.
Based on the results, an experimental method for determining the values is derived and validated in workbench measurements. This provides, for the first time, an easy-to-use method for determining the correct values of distributed capacitors.

I. INTRODUCTION

MR coils are a crucial part in the receiving chain of an MRI. Their characteristics determine the signal-to-noise-ratio (SNR) as well as the quality of the illumination of the volume-of-interest (VOI).
When the circumference of the conductor loop is comparable to the wavelength ($kb > 0.1$, with the wave number k and loop radius b), the resulting inhomogeneous current distribution leads to increasingly asymmetric profiles of the B_1^- (See Fig. 1). A well-known countermeasure to this is the use of distributed capacitors on the circumference of conductor loops (See Fig. 2). These compensate for the phase rotation of the current on the circumference and also lead to a quasi-static field distribution. With regard to transmit coils, they also lead to a reduced E-field, i.e. a reduced specific absorption rate (SAR) [1]. Although this measure is mentioned in numerous works, the author is not aware of any systematic framework to correctly determine the values of these capacitors [2], [3], [4]. Consequently, the values used in some papers appear to be determined heuristically or their dimensioning is difficult to comprehend [5]. Excepted from this are existing works on microstrip-line (MTL) coils, where the positive effect of distributed capacitors on their performance has already been addressed, including mathematical formalism to calculate correct values [6].

[1]Enrico Pannicke and Ralf Vick are with the Chair of Electromagnetic Compatibility, Otto-von-Guericke University Magdeburg, Germany enrico.pannicke@ovgu.de
[2] Oliver Speck is with the Chair of Biomedical Magnetic Resonance, Otto-von-Guericke University Magdeburg, Germany
[3] Enrico Pannicke and Oliver Speck are involved with Research Campus *STIMULATE*, Otto von Guericke University, Magdeburg, SA 39106, Germany

Therefore, the motivation of this work is to establish a systematic framework for the analysis of distributed capacitors on conductor loops. For this purpose, an analytical approach for the description of these conductor loops is developed and it is shown that the determination of the optimal values of the distributed capacitors is an eigenvalue problem. It is demonstrated that this insight provides a procedure for the experimental determination of the values, too.
The presented method and properties are validated experimentally and by means of numerical EM simulations.

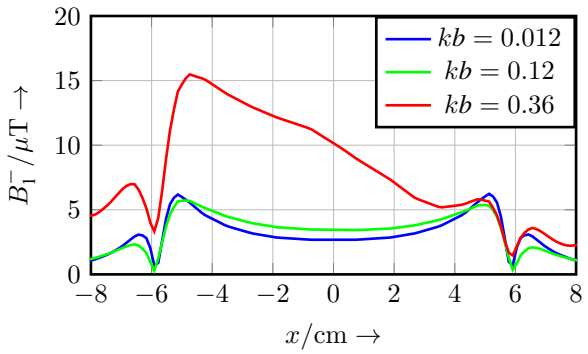

Fig. 1. Profile of the field beneath a 10 cm loop coil for a 1 A feed and different frequencies. As kb increases, the profile of the field distribution moves away from the "quasi-static" ideal.

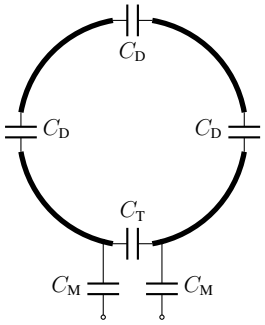

Fig. 2. Typical conductor loop with matching network and distributed capacitors on its perimeter.

II. THEORY

A. Admittance parameter

To calculate the required values for the distributed capacitors, a mathematical framework must be found for the setup in Fig. 2. For this purpose the admittance matrix was already identified by Harrington et. al. as a suitable framework [7]. Converting the conductor loop

into a four-pole representation requires the definition of N ports on a loop perimeter at $\varphi_\mathrm{n}; n = 1 \ldots N$. At each of these ports, the quantities $U_\mathrm{n} = U(\varphi_\mathrm{n})$ and $I_\mathrm{n} = I(\varphi_\mathrm{n})$ are defined according to Fig. 3. The geometry of the loop is given by it's center loop radius b and wire radius a. The corresponding admittance matrix $[\mathbf{Y}]$, with the dimension $(N \times N)$ is given by:

$$\begin{bmatrix} I_0 \\ I_1 \\ \vdots \\ I_{\mathrm{N\text{-}1}} \end{bmatrix} = \begin{bmatrix} Y_{11} & \ldots & Y_{1\mathrm{N}} \\ Y_{21} & \ldots & Y_{2\mathrm{N}} \\ \vdots & \ddots & \vdots \\ Y_{\mathrm{N}1} & \ldots & Y_{\mathrm{NN}} \end{bmatrix} \cdot \begin{bmatrix} U_0 \\ U_1 \\ \vdots \\ U_{\mathrm{N\text{-}1}} \end{bmatrix} \tag{1}$$

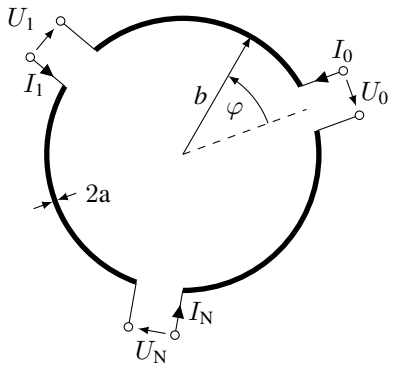

Fig. 3. Generalized arrangement describing a conductor loop with distributed two-ports along the circumference.

The known procedure for the determination of the $[\mathbf{Y}]$-parameters is used in particular by inserting short circuit conditions on all but one port of interest. Single parameter (f.ex. Y_{12}) can be calculated by the input admittance and current transfer functions [7] as shown below.
Applying the procedure described before Eq. 2 and Eq. 3 are retrieved to calculate the elements in Eq. (1).

$$Y_\mathrm{nn} = Y_\mathrm{IN}(\mathrm{a}, b) \tag{2}$$

$$Y_\mathrm{mn} = Y_\mathrm{IN}(\mathrm{a}, b) \cdot \frac{I_\mathrm{m}}{I_\mathrm{n}} \tag{3}$$

$Y_\mathrm{IN}(\mathrm{a}, b)$ is the input admittance of a loop coil with loop center radius b and wire radius a (see Fig. 3). Analytical expressions for $Y_\mathrm{IN}(\mathrm{a}, b)$ and ratio $I_\mathrm{m}/I_\mathrm{n}$ are available from [8]. These procedure is based on a fourier series evaluation with the coefficients $Z_{0,\mathrm{n}}$, which are given by [8]:

$$Z_{0,\mathrm{n}} = j2\pi\xi \cdot a_{0,\mathrm{n}} \tag{4}$$

ξ is the free space wave impedance and $a_{0,\mathrm{n}}$ can be derived from the geometrical characteristic of the loop analytically [9] or by a FFT-based algorithm [10].
If these are inserted into the computational rules for the main and side diagonals (Eq. (4) & Eq. (3)) and note that the calculation of the four-pole parameters is a cyclic permutation Eq. 5 and Eq. 6 are acquired.

$$Y_\mathrm{nn} = \frac{1}{Z_0} + 2 \cdot \sum_{k=1}^{\infty} \frac{1}{Z_\mathrm{k}} \tag{5}$$

$$Y_\mathrm{mn} = \frac{1}{Z_0} + 2 \cdot \sum_{k=1}^{\infty} \frac{\cos(k \cdot (\varphi_\mathrm{m} - \varphi_\mathrm{n}))}{Z_\mathrm{k}} \tag{6}$$

As Eq. (6) involves a cos-function, it is deduced that Eq. (6) and Eq. (5) are the Fourier series of an even function. By its symmetry one can prove that the $\mathbf{Y}$-matrix is symmetric along its main diagonal thus leading to $Y_\mathrm{mn} = Y_\mathrm{nm}$.

B. Eigenmode-Analysis

Due to the rotationally symmetrical arrangement of a conductor loop, it can be assumed that the values of the distributed capacitors are the same at a constant increment $\Delta\varphi$ between all ports. The relation between a port's current I_n and voltage U_n is determined by λ

$$\begin{bmatrix} I_0 \\ I_1 \\ \vdots \\ I_\mathrm{N} \end{bmatrix} = \lambda \cdot \begin{bmatrix} U_0 \\ U_1 \\ \vdots \\ U_\mathrm{N} \end{bmatrix} \tag{7}$$

and by this Eq. (1) is changed to

$$[\mathbf{Y}] \cdot [\mathbf{U}] = \lambda \cdot [\mathbf{U}] \tag{8}$$

. Therefore identifying the optimal values for the distributed capacitors is reduced to an eigenvalue-problem of the system matrix $[\mathbf{Y}]$. A $(N \times N)$ matrix contains N eigenvalues, thus the number of system modes is determined by the number of ports introduced: λ_i with $i = 0 \ldots (N-1)$.
Comparing Eq. (7) with Fig. 4 the port admittance Y_Pn required to obtain mode i can be identified with the eigenvalue λ_i by

$$Y_\mathrm{Pn}^\mathrm{i} = -\lambda_\mathrm{i} \tag{9}$$

and the input admittance Y_IN^i of the system terminated with Y_Pn^i is

$$Y_\mathrm{IN}^\mathrm{i} = \lambda_\mathrm{i} \tag{10}$$

The analytical calculation of the values of the distributed capacitors for the case of an equidistant placement of $\Delta\varphi = \pi$ on the conductor loop is outlined in the next section.

1) $\Delta\varphi = \pi$: In this case a (2×2)-matrix is derived

$$[\mathbf{Y}] = \begin{bmatrix} \frac{1}{Z_0} + 2 \cdot \sum_{k=1}^{\infty} \frac{1}{Z_\mathrm{k}} & \frac{1}{Z_0} + 2 \cdot \sum_{k=1}^{\infty} \frac{\cos(k \cdot \varphi_1)}{Z_\mathrm{k}} \\ \frac{1}{Z_0} + 2 \cdot \sum_{k=1}^{\infty} \frac{\cos(k \cdot \varphi_1)}{Z_\mathrm{k}} & \frac{1}{Z_0} + 2 \cdot \sum_{k=1}^{\infty} \frac{1}{Z_\mathrm{k}} \end{bmatrix}$$

, with its characteristic roots given by:

$$\lambda_0 = \frac{2}{Z_0} + 2 \cdot \sum_{k=1}^{\infty} \frac{(1 + \cos(k \cdot \varphi_\mathrm{k}))}{Z_\mathrm{k}} \tag{11}$$

$$\lambda_1 = 2 \cdot \sum_{k=1}^{\infty} \frac{(1 - \cos(k \cdot \varphi_\mathrm{k}))}{Z_\mathrm{k}} \tag{12}$$

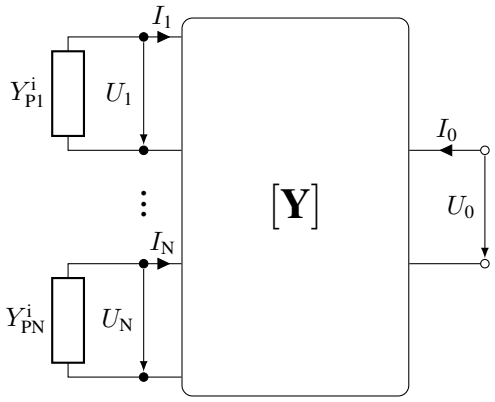

Fig. 4. Admittance matrix of the loop (compare Fig. 3) with port admittance's $Y_{\mathrm{P1}}, \ldots, Y_{\mathrm{PN}}$.

Just one of the two solutions is useful in application, as it corresponds to the homogeneous mode. To identify the proper solution the eigenvectors are determined by:

$$[[\mathbf{Y}] - \lambda \cdot [\mathbf{E}]] \cdot [\mathbf{U}] = 0.$$

It can be easily demonstrated that for $\lambda = \lambda_0$, $U_0 = U_1$ is obtained, which is clearly associated with the required solution. In contrast to this $\lambda = \lambda_1$ is leads to $U_0 = -U_1$, which is obviously maximizing the current variation on the loop.

The admittance to be used to compensate for any phase shift of the current distribution along the conductor loop is given by ($\lambda = \lambda_0$):

$$Y^0_{\mathrm{Pn}} = -\left(\frac{2}{Z_0} + 4 \cdot \sum_{k=1}^{\infty} \frac{1}{Z_{2\mathrm{k}}}\right) \tag{13}$$

In Fig. 5 calculated eigenvalues are shown as function of normalized wave number kb.

2) $\Delta\varphi = \pi/2$: In this case a (4×4)-matrix is retrieved:

$$[\mathbf{Y}] = \begin{bmatrix} Y_0 & Y_{\frac{\pi}{2}} & Y_{\pi} & Y_{\frac{3\pi}{2}} \\ Y_{\frac{3\pi}{2}} & Y_0 & Y_{\frac{\pi}{2}} & Y_{\pi} \\ Y_{\pi} & Y_{\frac{3\pi}{2}} & Y_0 & Y_{\frac{\pi}{2}} \\ Y_{\frac{\pi}{2}} & Y_{\pi} & Y_{\frac{3\pi}{2}} & Y_0 \end{bmatrix} \tag{14}$$

$$Y_0 = \frac{1}{Z_0} + 2 \cdot \sum_{k=1}^{\infty} \frac{1}{Z_{\mathrm{k}}}$$

$$Y_{\frac{\pi}{2}} = Y_{\frac{3\pi}{2}} = \frac{1}{Z_0} + 2 \cdot \sum_{k=1}^{\infty} \frac{\cos(k \cdot \pi/2)}{Z_{\mathrm{k}}}$$

$$Y_{\pi} = \frac{1}{Z_0} + 2 \cdot \sum_{k=1}^{\infty} \frac{\cos(k \cdot \pi)}{Z_{\mathrm{k}}}$$

The matrix in Eq. (14) is recognized to be a cyclic matrix, whose eigenvalues λ_{i} and eigenvectors U_{i} are determined by [11]:

$$\lambda_{\mathrm{i}} = Y_0 + Y_{\frac{\pi}{2}} \cdot w^{\mathrm{i}} + Y_{\pi} \cdot w^{2\mathrm{i}} + Y_{\frac{\pi}{2}} \cdot w^{3\mathrm{i}} \tag{15}$$

$$U_{\mathrm{i}} = \frac{1}{\sqrt{n}} \cdot \begin{bmatrix} 1 \\ w^{\mathrm{i}} \\ w^{2\mathrm{i}} \\ w^{3\mathrm{i}} \end{bmatrix} \tag{16}$$

, where $i = 0, 1, \ldots, 3$ and $w = \mathrm{e}^{\frac{j\pi}{2}}$. As before, only $i = 0$ represents the eigenvalue of the required mode, which is given by

$$Y^0_{\mathrm{Pn}} = -\left(\frac{4}{Z_0} + 8 \cdot \sum_{k=1}^{\infty} \frac{1}{Z_{4\mathrm{k}}}\right) \tag{17}$$

The derived formalism allows the analytical calculation of the required values for distributed capacitors under the condition that they are distributed with a constant increment $\Delta\varphi$ on a conductor loop.

C. Load Dependence

The properties of a coil changes significantly when it is loaded by the object of interest. Therefore, the question also arises with respect to the distributed capacitors, whether these show such a dependence, too.

As the validity of the eigenmode analysis is not touched by the loading - determining the correct values of the distributed capacitors is reduced to identifying the new representations of Z_{k}. According to An et.al. the coefficient in the presence of a lossy half-plane is identified by correcting Eq. (4) [12]:

$$Z_{\mathrm{k}} = j2\pi\xi \cdot (a_{\mathrm{k}} + b_{\mathrm{k}}) \tag{18}$$

The analytically calculated eigenvalues λ_0 for several increments $\Delta\varphi$ on a circular loop ($b = 57.5\,\mathrm{mm}$ and $a = 1.25\,\mathrm{mm}$) are shown in Fig. 5. For the loaded case a homogeneous phantom ($\epsilon_{\mathrm{r}} = 80$; $\sigma = 0.4\,\mathrm{S\,m^{-1}}$) was placed below the coil loop in a distance of $d = 5\,\mathrm{mm}$.

Fig. 6 shows the relative deviation caused by the presence of a phantom. It is evident that the deviation for $\Delta\varphi = \pi$ is further below $5\,\%$, which represents usual component tolerances. For $\Delta\varphi = \pi/2$ and $\Delta\varphi = \pi/4$ this limit is already reached at $kb = 0.3$.

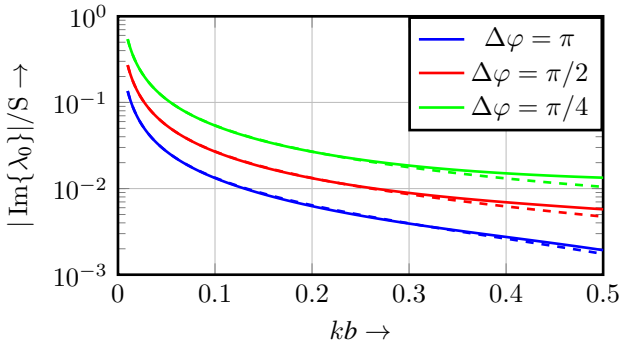

Fig. 5. Eigenvalue λ_0 of unloaded (line) and loaded (dashed) coil for different increments $\Delta\varphi$ in dependence of ratio kb.

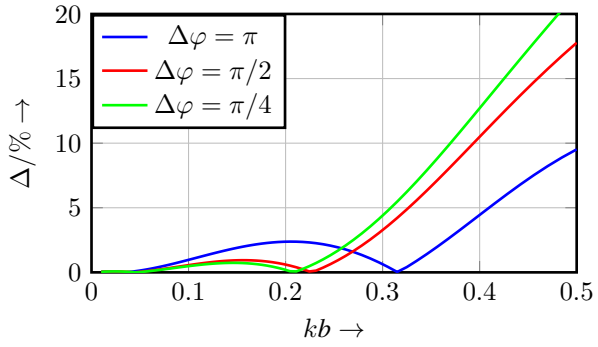

Fig. 6. Relative difference of the eigenvalues for the unloaded $\mathrm{Im}\{\lambda_0^{\mathrm{unload}}\}$ and loaded $\mathrm{Im}\{\lambda_0^{\mathrm{load}}\}$ setup $\Delta = |\mathrm{Im}\{\lambda_0^{\mathrm{unload}}\} - \mathrm{Im}\{\lambda_0^{\mathrm{load}}\}| / \mathrm{Im}\{\lambda_0^{\mathrm{unload}}\}$ for different increments $\Delta\varphi$ in dependence of ratio kb.

D. Experimental Determination

From Eq. (10) and Eq. (9) one can demonstrate that terminating the input admittance Y_{IN}^0 with Y_{Pn}^0 satisfies the series resonance condition. The minimized impedance of the loop is enhancing the inductive coupling to a probe as depicted in Fig. 7, showing the usual setup the determine distributed capacitors.
These already established procedure of placing capacitors C_{D} equidistant in the loop and vary their value until a resonance is measured at the intended frequency is in good agreement with the theoretical analysis.

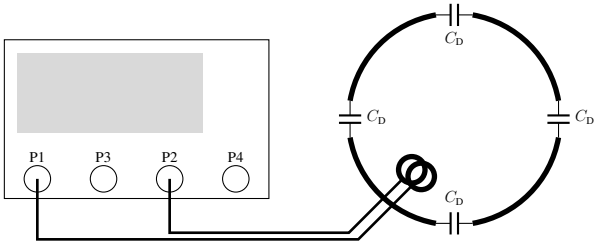

Fig. 7. Measurement setup to determine the distributed capacitors for a given conductor loop and target frequency.

III. Method

A. Admittance Parameter

To validate the mathematical framework the admittance matrix of a printed circuit loop was calculated ($b = 57.5\,\mathrm{mm}$ & $w = 2.5\,\mathrm{mm}$) and compared to numerical EM-simulations (openEMS, ATE - University of Duisburg-Essen, [13]). As the coefficients $a_{0,\mathrm{n}}$ is calculated for a round wire loop coil, the width w of the PCB-trace has to be converted to an effective radius by $a = w/4$ [14].
The admittance parameters were calculated by Eq. (5) and Eq. (6) with $\Delta\varphi = \pi$. From this the input impedance of two configurations could be deduced by means of a short circuit or open circuit on the second port.
Each configuration was analyzed for the unloaded and loaded case, where the latter compromised a lossy cylindrical phantom ($r = 1.5 \times b$ and $h = 20\,\mathrm{cm}$) below the coil, with an air gap in between of height $d = 5\,\mathrm{mm}$ ($\epsilon_{\mathrm{R}} = 80; \sigma = 0.46$).

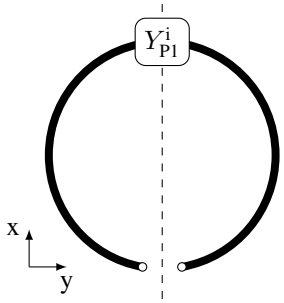

Fig. 8. Coil loop with an admittance $Y_{\mathrm{P1}}^{\mathrm{i}}$ located at $\Delta\varphi = \pi$.

B. Eigenmode-Analysis

To demonstrate the eigenmode-analysis the simulation results of the loaded coil from Sec. III-A were used. The resulting setup is shown in Fig. 8, with a summary of parameters to calculate the eigenvalues, as well as their values in Tab. I.
The coil's B_1^- was calculated along the x-axis (See Fig. 8 dashed line) [15].

w	5 mm	kb	0.36
b	57.5 mm	$\Delta\varphi$	π
Analytical			
$\mathrm{Im}\{\lambda_0\}$	−3.1283mS	$\mathrm{Im}\{\lambda_1\}$	2.7478mS
Simulation			
$\mathrm{Im}\{\lambda_0\}$	−3.1879mS	$\mathrm{Im}\{\lambda_1\}$	2.9349mS

TABLE I
Geometric parameters of the considered coil loop and calculated eigenvalues by Eq. (11) and Eq. (12) as well as extracted from the numerical results.

C. Experimental Determination

The experimental setup is depicted in Fig. 7. A circular loop with $b = 52.5\,\mathrm{mm}$, $w = 5\,\mathrm{mm}$ and $\Delta\varphi = \pi/2$ was constructed. The distance to the phantom ($\epsilon_{\mathrm{r}} = 80$ and $\kappa = 0.4\,\mathrm{S\,m^{-1}}$) was fixed to $d = 5\,\mathrm{mm}$.
Optimal values for the distributed capacitors were determined by the procedure outlined in II-D for the unloaded loop coil at $f = 123\,\mathrm{MHz}$. Measurements of S_{12} were performed for the unloaded and loaded loop coil to verify the predicted resonance.

IV. Results

A. Admittance Parameter

The results of the analytically calculated input impedance in comparison to simulation are shown in Fig. 9 and 10. For both configurations (open and short circuit) and different loading conditions very good agreement is achieved.
Although the analytical framework assumes a infinite half

plane [12] the impact of an finite phantom volume on the input impedance is correctly reproduced in terms of damping and frequency shift.

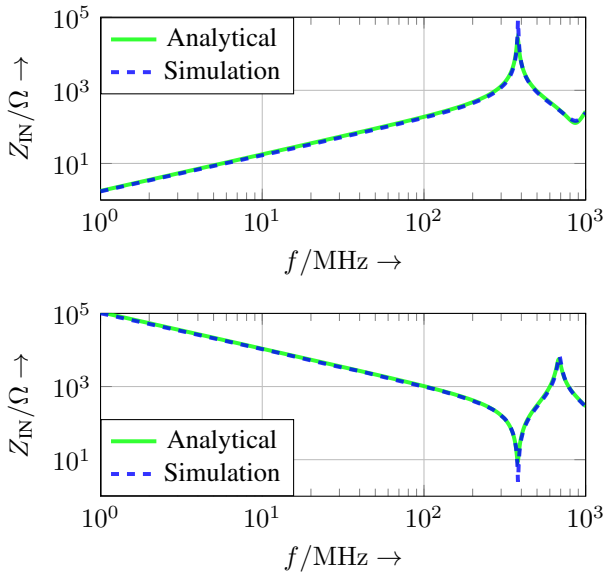

Fig. 9. Analytically calculated input impedance of a short circuit (top) as well as open circuit (bottom) coil loop compared to numerical results.

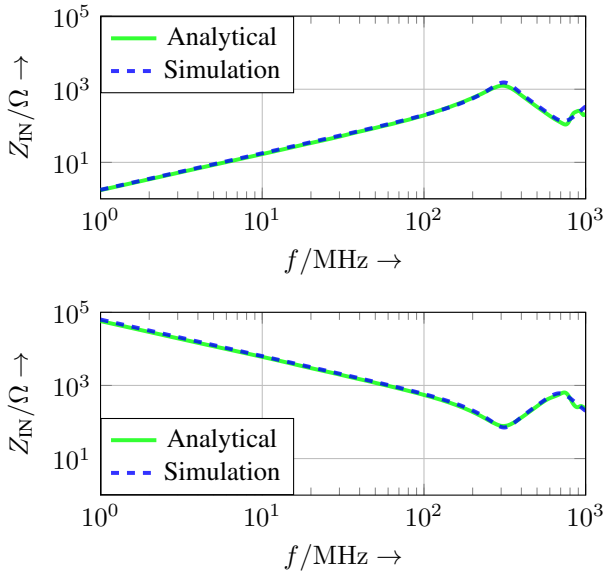

Fig. 10. Analytically calculated input impedance of a short circuit (top) as well as open circuit (bottom) coil loop loaded with a phantom in comparison to numerical results.

B. Eigenmode-Analysis

In Fig. 11 the results for the application of the admittance Y_{P1}^{i} in numerical simulations are shown in comparison to the initial case ($kb = 0.36$). The field profile for the initial case shows significant non-homogeneous profile, with an increase of amplitude of 300 % from right to left. For the homogeneous mode (λ_0) a quasi-static field distribution is obtained, with minimal variation of amplitude along the profile of 25 %. The so called "Anti-Mode" is received by applying λ_1.

The eigen-values λ_{i} calculated analytically and extracted from numerical results compare very well to each other (See Tab. I). The deviation for the homogeneous mode λ_0 is much smaller for the anti-mode λ_1.

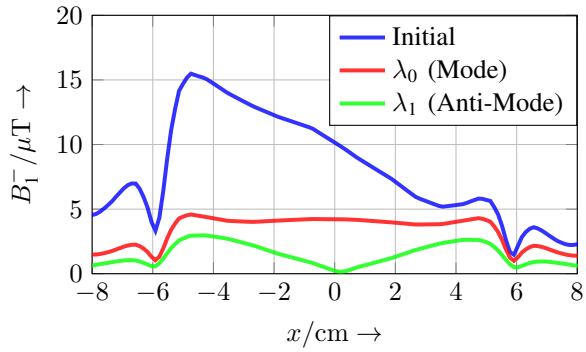

Fig. 11. Field profiles of a conductor loop for the case of different modes of current distribution determined by means of an eigenvalue analysis.

C. Experimental Determination

The distributed capacitors on an unloaded loop coil were calculated analytically to be $C_{\mathrm{D}} = 26.3\,\mathrm{pF}$ utilizing the formalism outlined in Sec. II-B.

The heuristic procedure outlined in Sec. II-D provided $C_{\mathrm{D}} = 27\,\mathrm{pF}$ as final result, which fits very well to the analytical results. The ratio $kb = 0.1357$ corresponds to $f = 123\,\mathrm{MHz}$ and is below the critical limit of $kb = 0.3$ (see Fig. 6). As demonstrated in Fig. 12 there is no apparent deviation between the loaded and unloaded coil. Both peaks are located at $f = 123\,\mathrm{MHz}$ with a significant drop of amplitude for the loaded coil.

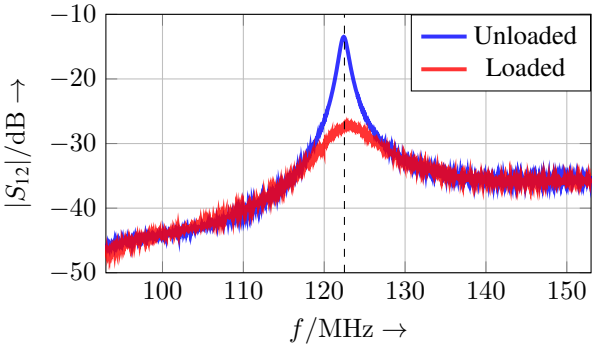

Fig. 12. Measurement to check the distributed capacitors.

V. DISCUSSION

The systematic analytical approach differs fundamentally from comparable rather heuristic works [5]. The presented method allows the correct analytical description of a conductor loop for the unloaded and loaded state. The formalism is based on approaches introduced by Wu et al.

[9] and has since been modified and extended for different configurations. For example, Jensen et.al. [16] introduced modifications which allow the calculation of rectangular or Huang et.al. [10] coupled conductor loops.

This provides a powerful approach for computing a wide variety of arrangements in MR receiving coils, and its applicability has been demonstrated for the first time in this work. Especially the correct analytical consideration of the loading allows to extract exact dimensions for components from this formalism.

Often the components values of a coil are found experimentally or numerically [17] [18]. Although this is a legitimate way of finding the result, the search space can be reduced enormously by the presented method and the number of repetitions can be reduced. The often encountered heuristic procedure in MR coil design could be greatly simplified in the case of distributed capacitors.

Since it has been shown that knowledge of the eigenvalues allows the input impedance to be determined, which can be expected for the tuning and matching networks of loaded coils, too. Corresponding investigations and comparisons are to be carried out next, as well as the consideration of coupled conductor loops.

The effect of the calculated eigenvalues was investigated using the field distribution of a single conductor loop in EM simulations. The insertion of the corresponding admittance can be used to generate the modes, whereas only the homogeneous mode seems to be useful in the application. For electrical large loops ($kb > 0.3$) inserting the distributed capacitors is providing a more homogeneous field profile, compared to the initial setup. But also for $kb < 0.3$ an improvement of the field profiles could be observed. Especially the center of the conductor loop seems to gain sensitivity. However, the difference is only $< 10\,\%$ and therefore might not play a role in practical application regarding performance optimization.

Analytical considerations of distributed capacitors for homogenization of current distribution and consequent improvement of sensitivity profiles is so far known only from microstrip-line (MTL) coils [6]. These insights will be used in future works to correlate the enhanced field profiles with sensitive maps of coils in the MR-Imaging. It is expected that the recorded maps will show a partially better but generally more homogeneous sensitivity, especially for larger loops.

ACKNOWLEDGMENT

The work of this paper is funded by the Federal Ministry of Education and Research within the Research Campus *STIMULATE* under grant number '13GW0473A'.

REFERENCES

[1] D. W. Alderman and D. M. Grant, "An efficient decoupler coil design which reduces heating in conductive samples in superconducting spectrometers," *Journal of Magnetic Resonance (1969)*, vol. 36, no. 3, pp. 447–451, 1979.

[2] D. Zhang and Y. Rahmat-Samii, "An ergonomie design for 3tesla mri neck coil," in *2016 IEEE International Symposium on Antennas and Propagation (APSURSI)*, pp. 463–464, 2016.

[3] J. R. Corea, A. M. Flynn, B. Lechêne, G. Scott, G. D. Reed, P. J. Shin, M. Lustig, and A. C. Arias, "Screen-printed flexible mri receive coils," *Nature communications*, vol. 7, no. 1, pp. 1–7, 2016.

[4] A. Gräßl, L. Winter, C. Thalhammer, W. Renz, P. Kellman, C. Martin, F. von Knobelsdorff-Brenkenhoff, V. Tkachenko, J. Schulz-Menger, and T. Niendorf, "Design, evaluation and application of an eight channel transmit/receive coil array for cardiac mri at 7.0t," *European Journal of Radiology*, vol. 82, no. 5, pp. 752–759, 2013.

[5] A. Hassan, I. Elabyed, J. Mallow, T. Herrmann, J. Bernarding, and A. Omar, "Optimal geometry and capacitors distribution of 7t mri surface coils," in *The 40th European Microwave Conference*, pp. 1437–1440, IEEE, 2010.

[6] V. Zhurbenko, "Optimal value of series capacitors for uniform field distribution in transmission line mri coils," *Journal of Sensors*, vol. 2016, 2016.

[7] R. F. Harrington and J. Mautz, "Electromagnetic behaviour of circular wire loops with arbitrary excitation and loading," *Proceedings of the Institution of Electrical Engineers*, vol. 115, no. 1, pp. 68–77, 1968.

[8] A. McKinley, *The Analytical Foundations of Loop Antennas and Nano-Scaled Rings*. Signals and Communication Technology, Springer Singapore, 2019.

[9] T. T. Wu, "Theory of the thin circular loop antenna," *Journal of Mathematical Physics*, vol. 3, no. 6, pp. 1301–1304, 1962.

[10] Yikun Huang, A. Nehorai, and G. Friedman, "Mutual coupling of two collocated orthogonally oriented circular thin-wire loops," *IEEE Transactions on Antennas and Propagation*, vol. 51, no. 6, pp. 1307–1314, 2003.

[11] G. J. Tee, "Eigenvectors of block circulant and alternating circulant matrices," 2005.

[12] L. N. An and G. S. Smith, "The horizontal circular loop antenna near a planar interface," *Radio Science*, vol. 17, pp. 483–502, May 1982.

[13] T. Liebig, "openems - open electromagnetic field solver."

[14] H. A. N. Hejase, "Analysis of a printed wire loop antenna," *IEEE Transactions on Microwave Theory and Techniques*, vol. 42, no. 2, pp. 227–233, 1994.

[15] D. I. Hoult, "The principle of reciprocity in signal strength calculations—a mathematical guide," *Concepts in Magnetic Resonance*, vol. 12, no. 4, pp. 173–187, 2000.

[16] M. A. Jensen and Y. Rahmat-Samii, "Electromagnetic characteristics of superquadric wire loop antennas," *IEEE Transactions on Antennas and Propagation*, vol. 42, no. 2, pp. 264–269, 1994.

[17] M. K. Chaubey, M. Gupta, R. Harsh, and T. Bhuiya, "Multi-channel hexagonal surface coils for 1.5t mri scanner," in *2016 International Conference on Communication Systems and Networks (ComNet)*, pp. 236–240, 2016.

[18] R. A. Lemdiasov and R. Ludwig, *A Standard Procedure for Analyzing Radio Frequency MRI Coils*. American Cancer Society, 2011.